Influence of Crystal Mosaicity on the X-Radiation Characteristics Observed at a Small Angle to the Particle Velocity Direction

D. A. Baklanov, I. E. Vnukov, Yu. V. Zhandarmov, G. T. Duong, S. A. Laktionova, and R. A. Shatokhin

Belgorod State University, Belgorod, Russia

Received November 16, 2010

Abstract—The experimentally measured yields of X-rays generated by 500-MeV electrons (the X-ray energies are $\omega \sim \gamma\omega_p$) in oriented tungsten single crystals are analyzed. A series of experiments have been performed at the Tomsk synchrotron with the use of crystal-diffraction spectrometers based on mosaic pyrolytic graphite crystals. The measured results are shown to be explained by competition between parametric X-radiation and bremsstrahlung diffraction in mosaic crystals of the $a\alpha$ class. The characteristic sizes of microblocks of refractory metal crystals are discussed from the standpoint of their influence on the positron yield in designed positron sources. A method for determining the characteristic sizes of microblocks in mosaic crystals of the $a\alpha$ class is proposed.

INTRODUCTION

Parametric X-radiation (PXR) is excited by the diffracted Coulomb field of a fast charged particle moving through a crystal [1–3]. Theory predicts that PXR reflections occur in the Bragg direction and, simultaneously, at small angles to the velocity of an emitting particle. However, if the first type of reflections has been investigated in detail, both theoretically and experimentally and demonstrated good agreement between experiment and theory [4, 5], PXR reflected at small angles to the particle velocity, which is sometimes referred to as forward PXR (FPXR), was discovered not so long ago in the experiments with tungsten crystals [6, 7] and silicon crystals [8] and still requires an adequate theoretical description. In [6, 9], various manifestations of this effect caused by a decrease in the photon energy [6] have been described qualitatively, but quantitative comparisons were not performed.

When the results of FPXR measurements are compared with theory, the basic difficulty consists in conventional PXR being emitted at large angles to the particle beam direction, separated rather easily from the bremsstrahlung background, and measured by ordinary X-ray detectors. Since transition radiation and bremsstrahlung propagate in the direction of FPXR reflections, this type of PXR can be extracted only with the help of crystal-diffraction spectrometers based on perfect silicon crystals [7, 8] and mosaic pyrolytic graphite (PG) crystals [6]. Their efficiency depends substantially on the spectral and angular distributions of radiation observed. Hence, direct comparison between measured results and calculations is impeded because calculations must be performed with allowance made for the actual characteristics of measuring equipment. An additional difficulty is that photons of bremsstrahlung and transition radiation can diffract in the crystal used to produce FPXR, thereby complicating the interpretation of measured results. From the foregoing, it follows that it is an important and urgent problem to analyze the influence of experimental conditions and bremsstrahlung photon diffraction on the radiation yield in the experimental investigations of FPXR, including [6, 7].

EXPERIMENTAL SETUP AND MEASUREMENTS

The experiment [6] is depicted schematically in Fig. 1. Electrons were accelerated up to the final energy $E_0 = 500$ MeV and directed to a single-crystal target mounted in a goniometer. X-rays under investigation passed through a collimator and a cleaning magnet and came into an experimental hall with recording equipment. To orient a crystal with respect to the direction of an electron beam, readings of a NaI(Tl) detector (the Compton kinematics) were used. The detector recorded photons with energy $\omega >$ 0.5 MeV in channeling radiation and bremsstrahlung after their scattering in converter S. Electron beam parameters, experimental equipment characteristics, and orientation methods are reported in [10, 11].

As was demonstrated in [13, 14], the optimal method of FPXR detection consists in measuring the dependence between the number of photons in a narrow spectral range and the crystal orientation. When photon energies are $\omega \geq 20$–25 keV, the Bragg condition can be satisfied only for several low-index planes

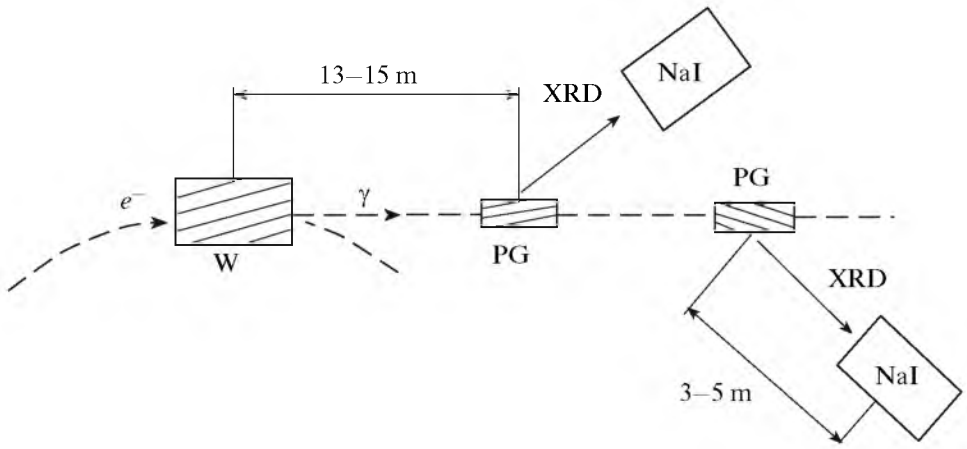

Fig. 1. Schematic representation of the experiment: W is the tungsten crystal, PG is the pyrolytic graphite crystal, NaI is the NaI(Tl) spectrometer, and S is the scatterer.

and a few totally defined crystal orientations. For photons with a fixed energy, the effect manifested itself as a peak in the orientation dependence (OD) of the photon yield, which was observed at the crystal orientation angles corresponding to Bragg reflection of radiation with this energy.

Fixed-energy radiation was extracted via two crystal-diffraction spectrometers based on mosaic PG crystals with sizes of 2.5 × 6.5 × 22.5 and 3.5 × 5.5 × 20 mm and NaI(Tl) detectors, each having a size of 40 × 1 mm. The spectrometers were mounted in goniometers at distances of 13–15 m from the tungsten crystal utilized to generate X-rays under investigation. Detectors and graphite crystals were 3–5 m apart. In graphite crystals, the mosaicity distributions were determined by measuring diffraction curves and identifying diffraction peaks for each of the detector's angular positions in the experiment [12]. In the thinner (2.5 × 6.5 × 22 mm) crystal, this distribution can be represented as a sum of two Gaussian distributions with the standard deviations $\sigma_m^1 = 4.2 \pm 0.1$ and $S_1 \sim 0.67 \pm 0.05$ mrad and the weighting coefficients $\sigma_m^2 = 9.0 \pm 0.5$ and $S_2 \sim 0.33 \pm 0.05$, respectively. Distribution centers coincide to an accuracy of 0.2 mrad or better. In another crystal, the mosaicity distribution can likewise be interpreted as a sum of two Gaussian distributions the respective parameters of which are $\sigma_m^1 = 6.2 \pm 0.4$ mrad, $S_1 \sim 0.64 \pm 0.05$, $\sigma_m^2 = 15.0 \pm 0.1$ mrad, and $S_2 \sim 0.36 \pm 0.05$. The shift between distribution centers is 10 ± 0.3 mrad.

Since detectors made of NaI(Tl) crystals 1 mm thick and differential discriminators were used, only the first allowed order of reflection was recorded, the background was substantially decreased, and the achieved peak/substrate ratio of diffraction curves was ~40–70, depending on the energy of recorded photons. In other words, the contribution of background photons with energies differing from the fixed value was less than 1.5–2%.

Under these conditions, the energy resolution of spectrometers weakly depends on the mosaicity of crystals and is determined by their angular apertures ($\Delta\Theta_x \sim 0.1$ and $\Delta\Theta_y \sim 0.6$ mrad) and the angle of collimation of diffracted radiation. In the diffraction (horizontal) plane, the radiation collimation angle was $\Delta\Theta_x = 0.4$–0.7 mrad, ensuring the spectrometer resolution $\Delta\omega/\omega \sim 1$–$2\%$. In [15], a new statistical simulation technique for calculating the spectrometer efficiency has been proposed. Based on the modified approach of [12], this technique made it possible to determine the spectral distributions of the efficiency of crystal-diffraction spectrometers, which were utilized for comparison of calculations with experimental results.

Measurements were performed for a tungsten single crystal having a size of 8.5 × 0.41 mm, the ⟨111⟩ orientation, and the surface mosaicity $\sigma_m \leq 0.2$ mrad. In crystals grown via the same technology, X-rays exhibited anomalous propagation through tungsten [16]. The crystal was mounted in the goniometer so that its $(11\bar{2})$ plane was arranged almost vertically. Such an arrangement enabled us to investigate the dynamic effects of radiation reflected from the $(11\bar{2})$ plane and two {110} ones rotated through an angle of 30° with respect to this plane. According to the ODs of the scattered photon yield measured under planar channeling [6], the angle between the $(11\bar{2})$ and vertical planes is $\beta = 3.5° \pm 0.2°$. Hence, for each of the crystal planes and the fixed photon energy, dynamic effects of X-rays were observed at different orientation angles.

As was predicted in [14], the FPXR intensity of a tungsten crystal is comparable with that of transition radiation only if the photon energy is $\omega \leq \gamma\omega_p \sim 80$ keV,

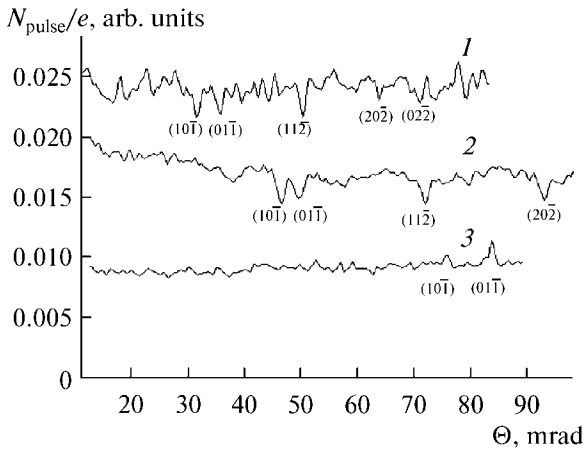

Fig. 2. X-ray yield ODs at the energies ω = (*1*) 95, (*2*) 67, and (*3*) 40 keV.

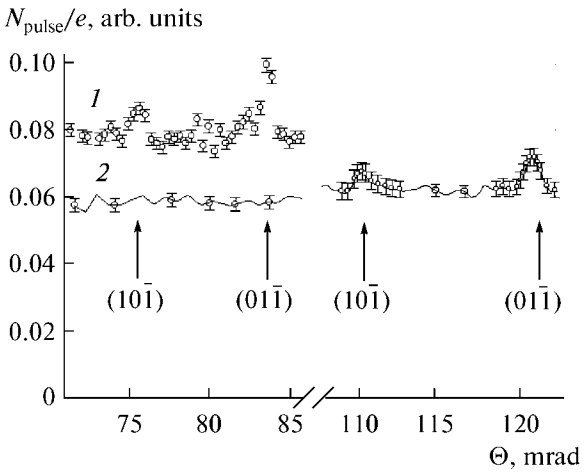

Fig. 3. X-ray yield ODs at the energies ω = (*1*) 40 and (*2*) 28.3 keV.

where γ is the Lorentz factor and ω_p is the plasma frequency of a medium. The latter must be proportional to the absorption length. Hence, in the first series of experiments, measurements were performed at the photon energies ω = 67 keV < $\gamma\omega_p$ and 95 keV > $\gamma\omega_p$. To ascertain that the radiation contribution is negligibly small under planar channeling, the yield of photons with ω ≥ 0.5 MeV was simultaneously measured by a Compton NaI(Tl) detector. The same detector was used to match the electron-beam direction to the crystal axis from which the angular disorientation between planes was counted off.

Measurements have not revealed peaks associated with FPXR at the chosen values of photon energy. At the given orientation of a tungsten crystal, a crystalline structure manifested itself as a decrease in the number of photons if the Bragg energy fitted the energy to which crystal-diffraction spectrometers were tuned. The positions of the OD minima correspond to the kinematic diffraction conditions for photons emitted along the electron beam direction. In this case, the error does not exceed 1%. For example, when ω = 67 keV and reflections occur from the $(10\bar{1})$, $(01\bar{1})$, and $(11\bar{2})$ planes, the calculated positions of OD minima are 46.6, 49.9, and 72.2 mrad. In this case, the measured values are 46.3, 49.5, and 71.9 mrad. The depth of minima varies from 12–15 (ω = 67 keV) to ~10% (ω = 90 keV). The typical full width of a minimum is $\Delta\Theta \sim 15$–2.5 mrad. In other words, the ODs of the high-energy photon yield have dips caused by bremsstrahlung diffraction inside the crystal.

FPXRs were revealed only for low photon energies ω = 40 (Fig. 2, curve *3*; Fig. 3) and 28.3 keV, at which the positions of maxima, similarly to those of the minima in the yields of high-energy photons, obey Bragg's law. The observed maxima are not related to any continuous radiation or an experimental error. This is confirmed by the fact that the yield of photons with ω ≥ 0.5 0.5 MeV has no maxima ([6]; Fig. 3) and the OD of the X-ray photon yield exhibits different positions of maxima at different photon energies. The position and shape of maxima remained unchanged in repeated measurements. Analogous results, i.e., the OD dip corresponding to the photon energy ω = 120 keV ~ $\gamma\omega_p$ ~ 134 keV and its peak occurring at ω = 40 keV < $\gamma\omega_p$, have been obtained in the subsequent experiment [7] performed at the electron energy E_0 = 885 MeV.

For ω = 40 keV, the diffracted radiation spectra were measured at the peak point ($\Theta^{exp}_{01\bar{1}}$ = 83.9 mrad) and at the neighboring points (Θ = 81.3 and 79.3 mrad). As was ascertained, the radiation intensity increases exclusively at the first order of reflection. All spectral intensities corresponding to the higher orders of reflection have identical values.

When the photon energy is ω = 40 (28.3) mrad, the recorded positions of peaks, $\Theta^{exp}_{10\bar{1}}$ = 76.6 (110.2) and $\Theta^{exp}_{01\bar{1}}$ = 83.9 (120.9) mrad, differ slightly from the estimated values, $\Theta^{est}_{10\bar{1}}$ = 77.9 (110.2) and $\Theta^{est}_{01\bar{1}}$ = 83.6 (118.2) mrad. The interpeak distances are 1.5 and 2 mrad greater than those expected according to Bragg's law. At the aforementioned two values of photon energy, the peak width for the $(01\bar{1})$ plane is nearly twice as large as that for the $(10\bar{1})$ plane. When ω = 40 mrad, this peak is divided rather reliably into two parts.

ANALYSIS OF THE MEASURED RESULTS AND CONCLUSIONS

From the theoretical standpoint, the FPXR energy is determined by the angle $\Theta_{||}$ of photon emission perpendicular to the reflection plane. Its intensity is zero strictly along the electron velocity, and the maximum of an angular distribution corresponds to the angle

$\Theta_{\parallel}^{FPXR} = \frac{1}{\sqrt{3}}\sqrt{\gamma^{-2} + (\omega_p/\omega)^2}$. In the experiment under analysis, recorded photons were induced by electrons moving at an angle of approximately Θ^{FPXR} with respect to the electron-beam direction. X-rays were generated on tungsten crystal planes rotated through an angle of ~30° with respect to the reflecting plane of diffractometers. In combination with the finite angular aperture and resolution of spectrometers, these conditions must have led to wider experimental curves and lower peak amplitudes than those described by the theory not defining their influence.

Since the photon yields were measured simultaneously at energies $\omega > \gamma\omega_p$, at which the main mechanism of forming an observed OD is bremsstrahlung diffraction, and in the energy range below this level, where two mechanisms can be expected to manifest themselves [6, 9]), it is possible to consider the contribution of bremsstrahlung diffraction at photon energies $\omega < \gamma\omega_p$.

The calculated ODs of the forward yield of X-rays are depicted in Fig. 4. In calculations performed under the conditions of experiment [6], the efficiency of spectrometers and the contribution of transition radiation from the rear crystal face were taken into account. The angular range of crystal disorientation was 30–120 mrad, and photon energies were ω = 96, 67, 40, and 28.3 keV (curves *1–4*, respectively). The technique for estimating the approximate contribution caused by diffraction suppression of the radiation yield is reported in [17].

Comparison of the experimental and calculated X-ray yields (table) confirms the adequacy of calculations.

The error of absolutization of experimental data is ~15%. The results were obtained immediately from the measured ODs of radiation yields (at photon energies of 96, 67, 40, and 28.3 keV) and according to X-ray spectra (at photon energies of 80 and 120 keV) for a single orientation of the graphite crystal with respect to the diffracted-radiation detector and several orders of reflection. In the measured yields, the NaI(Tl) spectrometer efficiency calculated via the Monte Carlo method and the radiation absorption both in the output flange of an accelerator and in the air space between an accelerator and a detector were taken into account. Calculations were performed by allowing for the crystal-diffraction spectrometer efficiency, bremsstrahlung suppression owing to the density effect [18], X-ray absorption in the tungsten crystal, and the contribution of transition radiation from the output face of a target.

As can be seen in Fig. 4, the dip depths of OD curves calculated for the {110} planes are ~2.5 and ~1.5% at photon energies of 67 and 96 keV, respectively; i.e., they are less than the experimental dips (~15 and ~10%, respectively) by a factor of about 5. The widths of calculated curves are less than those of

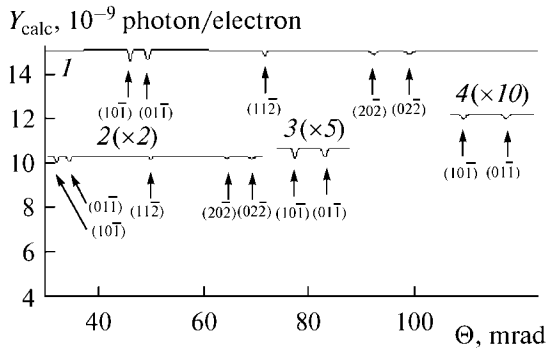

Fig. 4. Calculated dependences of the X-ray yield at the energies ω = (*1*) 96, (*2*) 67, (*3*) 40, and (*4*) 28.3 keV.

the measured curves (Fig. 2) by a factor of approximately 1.2–1.5. At the given level of statistics, such dips can hardly be identified in experimental dependences. The positions of observed dips agree fairly well with calculations, including the dip positions corresponding to weakly reflecting (11$\bar{2}$) and (220) planes (Figs. 2, 4). As in the case of strongly reflecting planes, the depths of experimental dips exceed those of calculated dips by a factor of 5–7.

In the previously developed technique [17], the influence of absorption on a diffraction process is not considered [19]. However, with allowance for this phenomenon, dips can become only somewhat wider and the reflection efficiency (their depth) remains absolutely unchanged, as is evidenced by estimates. In the calculated results, the diffraction effect is insignificant, because the difference between the characteristic width of a total reflection region (~30–40 eV) and the energy range of a spectrometer (~0.5–1.5 keV, depending on the recorded radiation energy) is large.

Compared to perfect crystals, mosaic ones are known to reflect X-rays to a greater extent [19]. This feature explains relatively deep dips in the measured ODs of the radiation yield. On the other hand, the

Comparison of the experimental and calculated X-ray yields

ω, keV	Y_{exp}, photon/electron	Y_{calc}, photon/electron	Y_{exp}/Y_{calc}
28.3	1.16×10^{-9}	1.27×10^{-9}	0.96
40	1.99×10^{-9}	2.13×10^{-9}	0.95
67	14.78×10^{-9}	15.5×10^{-9}	0.95
80	0.40×10^{-9}	0.36×10^{-9}	1.1
96	5.1×10^{-9}	5.15×10^{-9}	0.99
120	3.6×10^{-10}	3.47×10^{-9}	1.04

experiment under consideration exhibited, for the first time, the dynamic effect of radiation from fast electrons in crystals, undoubtedly indicating the perfect structure of a crystal. The best way out of such a situation is to assume that dynamic effects can also manifest themselves in X-rays reflected from mosaic crystals [19]. This assumption is valid only if perfectly structured blocks have sizes greater than the primary extinction length (in our case, ~2–3 μm).

As was found in the monograph cited above, a mosaic crystal is superior to a perfect one in X-ray reflection efficiency if the conditions $l > l_{ex}$ and $l < l_a$, (l is the block size, l_{ex} is the primary extinction length, and l_a is the photon absorption length) hold simultaneously. This relation was observed in [6, 7]. According to the accepted terminology [19], such a crystal belongs to the $a\alpha$ class. One of the confirmations of this classification is the small surface mosaicity $\sigma_m \approx 0.2$ mrad. As is known, standard methods of X-ray diffraction analysis are incapable of determining the quality of the internal structure of samples with commensurate thicknesses and compositions. Hence, it can only be assumed that the internal part of a crystal must have approximately the same mosaicity. Another confirmation is the dip-free yields of high-energy photons with energies $\omega > \gamma\omega_p$ observed at a significantly smaller statistical error in an experiment [13] in which the same recording equipment and the identical measurement technique were used to investigate the dependence between the fixed-energy radiation yield and the orientation of a perfect silicon crystal.

When several microblocks are rotated through small angles with respect to the average direction, a crystal-diffraction spectrometer detects photons with an increased probability of reflection. Hence, the dip depth grows. As an estimate suitable for determining the maximally possible diffraction loss of the radiation yield, the ratio between the average absorption length and the average size of a microblock can be chosen. From this estimate and experimental data obtained at the photon energy $\omega = 67$ keV ($l_a \sim 183$ μm), the average size of the block of a tungsten crystal is ~20–30 μm. In the experiments [6, 7], the measured surface mosaicity of the crystal ($\sigma_m \approx 0.2$ mrad) is small and comparable with the Darwin table width $\Delta\Theta \sim 0.03$ mrad [19]. Hence, rereflected diffracted X-rays should be observed. Therefore, the actual number of blocks required to ensure the experimentally determined diffraction suppression of the radiation yield becomes greater, with the average size of a block decreasing accordingly.

In the experimental OD of the yield of photons with $\omega = 40$ keV [6], there is no dip because the FPXR contribution compensates for the radiation yield loss arising from bremsstrahlung photon diffraction inside the crystal at energies $\omega < \gamma\omega_p$ [9]. As was shown in [20], the crystal mosaicity hardly affects the total yield of PXR at all. Therefore, it can be assumed that the FPXR yield also remains unchanged because the crystal mosaicity $\sigma_m \approx 0.2$ mrad is substantially less than the characteristic angle of emission of FPXR photons ($\Theta_{\parallel}^{FPXR} = \frac{1}{\sqrt{3}}\sqrt{\gamma^{-2} + (\omega_p/\omega)^2} \sim 1.3$ mrad). A more valid answer to this question requires comprehensive theoretical analysis.

At photon energies $\omega = 40$ and 28.3 keV, the measured and calculated radiation yields agree well beyond the region of diffraction effects, making it possible to estimate the FPXR yield of a tungsten crystal under conditions of the experiment [6]. When the photon energy is $\omega = 40$ (28.3) keV, the spatial angle is $\Delta\Omega = 2.02 \times 10^{-7}$ sr, and the spectrometer's energy capture is $\Delta\omega = 0.276$ (0.172) keV (the full width at half maximum), the observed FPXR yield reaches ~28% (~20%) of the total yield of bremsstrahlung and transition radiation. At the photon energy $\omega = 28.3$ keV, the ratio between the yields of FPXR and the sum of bremsstrahlung and transition radiation is smaller because the contribution of transition radiation from the crystal's output face to the total yield of recorded radiation is higher (~68%) than in measurements with energy $\omega = 40$ keV (~20%).

At the photon energy $\omega = 40$ keV ($l_a \sim 48$ μm), the dip depth is estimated to be the same or larger (Fig. 4) owing to bremsstrahlung diffraction. Therefore, at the photon energy $\omega = 40$ keV, the observed OD (Fig. 3, curve *1*) is the sum of the wider OD of the photon yield generated by the FPXR mechanism (its amplitude is approximately half as high again or twice as high as the experimentally recorded amplitude) and the OD caused by diffraction suppression. It is evident that the same cause leads to different shapes of the ODs of the FPXR yield from physically identical $(10\bar{1})$ and $(01\bar{1})$ planes [6] (Fig. 3). Since the $(10\bar{1})$ plane has a smaller angle with the analyzer's crystal, the dip of the high-energy photon yield is deeper and narrower than the OD dip inherent to the $(01\bar{1})$ plane rotated through a larger angle (Fig. 2). Hence, the amplitude of its resulting dependence is half as much. In other words, when there is no diffraction suppression in the mosaic crystal of $a\alpha$ class (i.e., in the tungsten crystal), the FPXR yields corresponding to conditions of the experiment [6] must be about 50 and 30–40% at photon energies of 40 and 28.3 keV, respectively.

Under conditions of the experiment [7] with the same tungsten crystal, the situation is somewhat different. The electron energy was increased from 500 to 855 MeV. Hence, the total yield of radiation with $\omega =$ 40 keV contained only ~30% of bremsstrahlung and the observed radiation yield decreased by 10% or less.

The results discussed above make it possible to propose a new method for estimating the structural quality of crystals with large thicknesses, which relies on determining the degree of PXR reflections along the

particle velocity at photon energies $\omega < \gamma\omega_p$ and the bremsstrahlung diffraction in the range of $\omega > \gamma\omega_p$. A perfect crystal must exhibit predominant FPXR and negligibly low bremsstrahlung suppression. On the contrary, in a *b*-class mosaic crystal, i.e., in a crystal with a typical microblock size less than the primary extinction length, bremsstrahlung suppression must play an appreciable role and FPXR disappears. It is evident that the size of perfect blocks can also be estimated by measuring the FPXR yields at weaker orders of reflections: 220, 440, etc. According to the dynamic theory of X-ray diffraction, the extinction length corresponding to such reflections increases. Hence, if FPXR disappears at a certain order of reflections, the average size of perfect blocks is less than l_{ex} inherent to these reflections.

The proposed method for estimating the average microblock size can be implemented by performing measurements under the condition that photon energies are $\omega \sim \gamma\omega_p$ or less. On the other hand, it is necessary to operate with photons with absorption lengths that substantially exceed the primary extinction length. To ensure simultaneous fulfillment of these conditions, especially in the case of crystals made of heavy elements, measurements must be performed at accelerators with energies of 1 GeV or higher, which often prove to be economically unprofitable. To perform such investigations with accelerators of moderate energy (~20–30 MeV), it is possible to use the ratio between the experimentally measured diffraction suppression and its calculated value. The main requirement is that bases must be long enough to implement extraction of fixed-energy radiation via a crystal-diffraction spectrometer based on a perfect or mosaic crystal.

The most interesting application of radiation from relativistic electrons moving through crystals is its utilization to generate intense positron beams [21]. At present, positron beams are produced with the help of cascade processes in refractory metal targets irradiated by relativistic electron beams. However, this technique cannot ensure the required yield of positrons owing to high energy release capable of melting a target. In connection with the beginning of the construction of linear electron–positron colliders, this problem is most topical because the collider efficiency is proportional to the number of interacting particles.

For this purpose, tungsten crystals with the ⟨111⟩ orientation are assumed to be most optimal. Their thicknesses are several millimeters, depending on the electron energy. In experiments performed with electron beams having energies from 1 to 8 GeV and tungsten crystals, it was revealed that crystals are really more efficient than polycrystalline targets of an optimal thickness and ensure an increase in the positron yield by 15–30% at electron energies exceeding 4–5 GeV [22]. The basic sources of photons generating electron-photon pairs are channeling and above-barrier radiations and coherent bremsstrahlung. The calculated ODs of the positron yield obtained for the crucial contribution of the latter radiation mechanism [23] agree rather well with the measured results [22].

The imperfection of crystal structures (the disorientation of perfect blocks of a sample with respect to the reference direction and their limited sizes) suppresses the coherent effects of radiation. Owing to these effects, crystals are advantageous over amorphous radiators in positron generation. The modern technique for fabricating crystals from refractory metals (W and Mo) cannot ensure their perfect structures. (In experiments with positron generation, the surface mosaicity of samples was $\sigma_m \sim 0.5–1.5$ mrad, i.e., significantly exceeded characteristic radiation angle $\gamma^{-1} \sim$ 0.1 mrad at electron energies on the order of several gigaelectronvolts.) Hence, verification of the internal structure of these crystals is an impotent and urgent problem. It should be noted that the yields of radiation induced by interaction of fast electrons with oriented crystals were calculated, until recently, without allowance for structural imperfection.

Estimates indicate that the main parameter capable of leading to radiation yield suppression is the characteristic size of mosaic blocks. Suppression starts if the block size becomes comparable to radiation formation length $l \sim l_{coh} = \gamma^2\lambda$, where λ is the photon wavelength. When the photon energies required to produce positrons with desired energies (5–20 MeV) is 10–150 MeV and the electron energy ~ 5 GeV, $l_{coh} \approx 2–20$ μm. The influence of disoriented neighboring blocks is substantially weaker and, in the first approximation, can be ignored. Hence, the proposed methods for estimating the sizes of blocks of such crystals are of great importance from the standpoint of the development of new-generation positron injectors.

ACKNOWLEDGMENTS

We thank our colleagues [6] for participation in the development and implementation of the techniques used in investigations and their assistance in measurements.

This study was supported in part by the Scientific and Scientific-Pedagogical Personnel of Innovative Russia Federal Targeted Program (state contract no. 16.740.11.0147 dated September 2, 2010) and the Program of Internal Grants of Belgorod State University (grant no. VKG 002.10).

REFERENCES

1. M. L. Ter-Mikaelyan, *The Influence of the Medium on High-Energy Electromagnetic Processes* (Akad. Nauk ARM SSR, Yerevan, 1969) [in Russian].
2. G. M. Garibyan and Yan Shi, Zh. Eksp. Teor. Fiz. **61**, 930 (1971) [Sov. Phys. JETP **34**, 595 (1971)].
3. V. G. Baryshevskii and I. D. Feranchuk, Zh. Eksp. Teor. Fiz. **61**, 944 (1971) [Sov. Phys. JETP **34**, 502 (1971)].

4. V. G. Baryshevskii and I. Ya. Dubovskaya, in *Results of Science and Engineering, Ser. Beams of Charged Particles and Solid* (VINITI, Moscow, 1991), Vol. 4, p. 129 [in Russian].
5. K.-H. Brenzinger, C. Herberg, B. Limburg, et al., Z. Phys. A **358**, 107 (1997).
6. A. N. Aleinik, A. N. Baldin, E. A. Bogomazova, et al., Pis'ma Zh. Eksp. Teor. Fiz. **80**, 447 (2004) [JETP Lett. **80**, 393 (2004)].
7. H. Backe, W. Lauth, A. F. Scharafutdinov, et al., Proc. SPIE–Int. Soc. Opt. Eng. **6634** (2006), arXiv:physics/06099151 v1 (2006).
8. H. Backe, A. Rueda, W. Lauth, et al., Nucl. Instrum. Methods. Phys. Res. B **234**, 130 (2005).
9. V. Likhashev, N. Nasonov, A. Tulinov, and R. Zhukova, Vestn. Voronezh. Univ., Ser. Fiz. Matem., No. 2, 98 (2005).
10. Yu. N. Adishchev, S. A. Vorob'ev, V. N. Zabaev, et al., Yad. Fiz. **35**, 108 (1982) [Sov. J. Nucl. Phys. **35**, 63 (1982)].
11. B. N. Kalinin, E. I. Konovalova, G. A. Pleshkov, et al., Prib. Tekh. Eksp., No. 3, 31 (1985).
12. I. E. Vnukov, B. N. Kalinin, A. A. Kir'yakov, et al., Izv. Vyssh. Uchebn. Zaved., Ser. Fiz. **44** (3), 71 (2001).
13. B. N. Kalinin, G. A. Naumenko, D. V. Padalko, A. P. Polylitsyn, and I. E. Vnukov, Nucl. Instrum. Methods. Phys. Res. B **173**, 253 (2001).
14. A. Kubankin, N. Nasonov, V. Sergienko, and I. Vnukov, Nucl. Instrum. Methods. Phys. Res. B **201**, 97 (2003).
15. D. A. Baklanov, I. E. Vnukov, Yu. V. Zhandarmov, et al., in *Proceedings of the 40th Intern. Conference on Physics of Interaction of Charged Particles with Crystals* (Mosc. Gos. Univ., Moscow, 2010), p. 94.
16. I. K. Bdikin, S. I. Bozhko, V. N. Semenov, et al., Pis'ma Zh. Tekh. Fiz. **25**, 16 (1999) [Tech. Phys. Lett. **25**, 598 (1999)].
17. D. A. Baklanov, A. N. Baldin, I. E. Vnukov, D. A. Nechaenko, and R. A. Shatokhin, Vestn. Khark. Nats. Univ., Ser. Fiz. **763** (1), 41 (2007).
18. V. P. Kleiner, N. N. Nasonov, and N. A. Shlyakhov, Ukr. Fiz. Zh. **57**, 48 (1992).
19. R. W. James, *The Optical Principles of the Diffraction of X-Rays*, revised ed. (Bell, London, 1962; Mir, Moscow, 1966).
20. A. M. Afanas'ev and M. A. Aginyan, Zh. Eksp. Teor. Fiz. **74**, 570 (1978) [Sov. Phys. JETP **47**, 300 (1978)].
21. R. Chehab, F. Couchot, A. R. Nyaieh, F. Richard, and X. Artru, LAL-RT 89-01 (1989).
22. T. Suwada, S. Anami, R. Chehab, et al., Phys. Rev. E **67**, 016502 (2003).
23. B. N. Kalinin, G. A. Naumenko, A. P. Potylitsin, et al., Nucl. Instrum. Methods. Phys. Res. B **145**, 209 (1998).